Science Advances
AAAS

advances.sciencemag.org/cgi/content/full/5/9/eaax4545/DC1

# Supplementary Materials for

## Ultrafast optical field–ionized gases—A laboratory platform for studying kinetic plasma instabilities

Chaojie Zhang*, Chen-Kang Huang, Ken A. Marsh, Chris E. Clayton, Warren B. Mori, Chan Joshi*

*Corresponding author. Email: chaojiez@ucla.edu (C.Z.); cjoshi@ucla.edu (C.J.)

Published 6 September 2019, *Sci. Adv.* **5**, eaax4545 (2019)
DOI: 10.1126/sciadv.aax4545

**This PDF file includes:**

**Supplementary Text**

**Supplementary Text and Figures**

**The streaming instability start to grow from the outer edge of the plasma in the LP case**

In the LP case, the streaming instability is driven by streams formed by reflection of the hot $He^{2+}$ electrons from the sheath, therefore the instability starts to grow from the outer edge of the plasma and propagates inwards. This is clearly illustrated in fig. S1 where snapshots of density fluctuations within a fixed spatial region in the simulation box from t=0.9 ps to t=1.9 ps are shown.

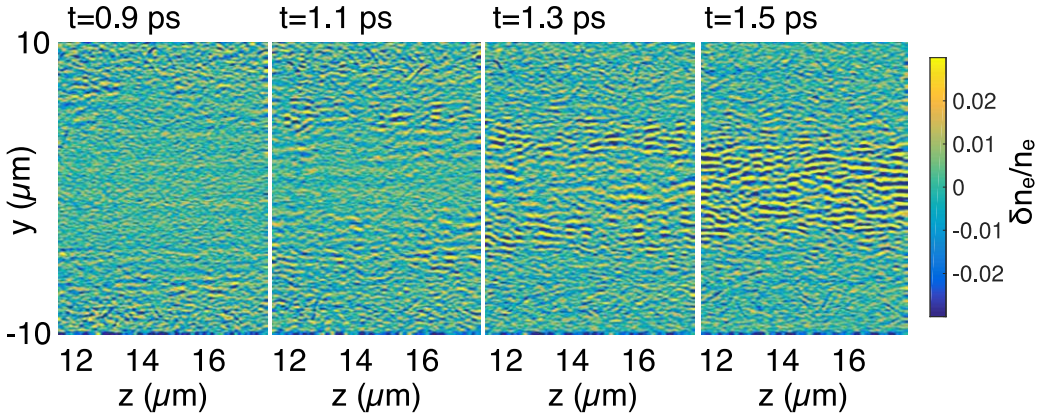


**Fig. S1. A time sequence of snapshots of electron density fluctuations.**

**PIC simulation including ionization and e-e collisions**

Although we have shown in the main text that within the first few ps, the evolution of the OFI plasma is dominated by kinetic instabilities and that e-e collisions play negligible roles in isotropizing/thermalizing the plasma, here we show the results of a 2D PIC simulation which self-consistently includes both ionization and e-e collisions.

Figure S2A and B show the amplitude spectral density of the density fluctuations in 2D simulations without and with e-e collisions, respectively. A notable difference is that the instabilities with large wavenumbers are suppressed by collisions which is expected. For the instabilities with relatively small wavenumbers (e.g., $k < 2k_0$), the effects of collisions are insignificant. Figure S2C shows $\delta n_e(k)$ as a function of time, where $k = (k_y = -k_0, k_z = 1.7k_0)$ is the wavenumber that being measured in the experiment (the CP case). It can be seen that the inclusion of collisions slightly reduces the growth rate of the instability. Nevertheless, the overall shape of the two curves are very similar.

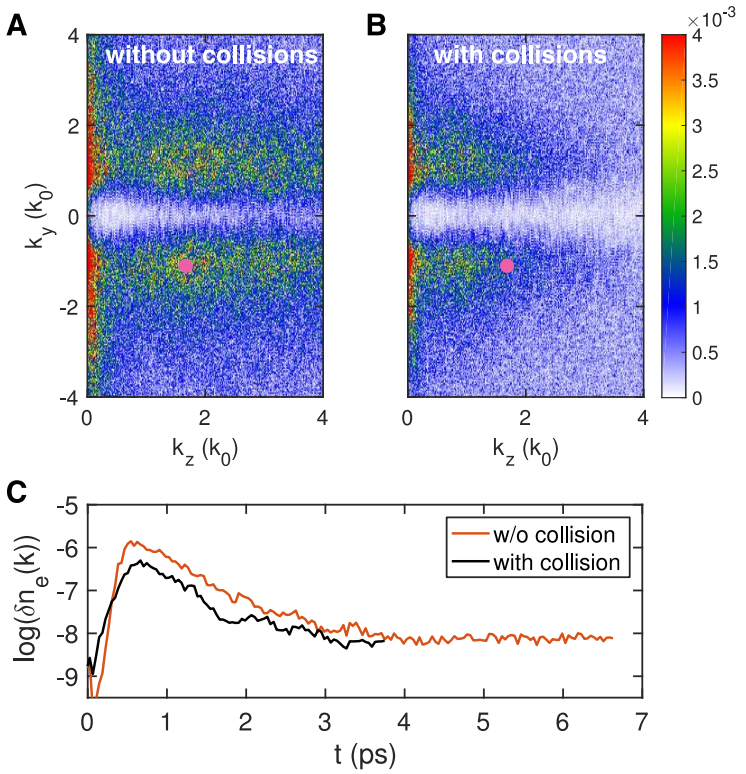


**Fig. S2. Comparison of PIC simulations without and with e-e collisions.** The $k$ space of the density fluctuation in (**A**) and (**B**) are taken at 0.6 ps. The red dots mark the measured $k = (k_y = -k_0, k_z = 1.7k_0)$ in the experiment (the blue satellite in the CP case). (**C**) shows $\delta n_e$ at the measured $k$ as a function of time.

**<u>Relaxation of two groups of electrons due to collisions</u>**

The thermalization of the electrons due to e-e collisions in the PIC code has been extensively checked to ensure that the isotropization of the electron distributions is dominated by kinetic effects. Here we show two examples in fig. S3. The first example is the relaxation of four drifting Maxwellian beams. The parameters of the beams are similar to those of the OFI plasma ionized by a CP laser: $n_1 = n_2 = 0.375n_0$, $n_3 = n_4 = 0.115n_0$, where $n_0 = 5 \times 10^{18}$ cm$^{-3}$ is the total plasma density. The drift velocities of the beams are $v_1 = -v_2 = 0.0204c$, $v_3 = -v_4 = 0.0616c$. The temperatures in the drift direction are $T_{\perp 1} = T_{\perp 2} = 97$ eV and $T_{\perp 3} = T_{\perp 4} = 44$ eV. The temperatures in the directions orthogonal to the drift direction are $T_{\parallel 1,2,3,4} = 1$ eV. Although each beam itself is relatively cold in the drift direction, the rms temperature of the plasma is large (695 eV) due to the drifts of the beams. The simulation box has dimensions of $1 \times 1\ c/\omega_p$ and is divided into $48 \times 48$ cells. 256 particles are initialized in each cell.

The solid lines in fig. S3A show the rms temperature of the plasma in the drift direction (red) and that in the orthogonal direction (blue). The black dashed lines show the expected temperatures calculated using the NRL formula by assuming that the plasma is anisotropic and has temperatures of 695 eV and 1 eV in the hot ($\perp$) and the cold ($\parallel$) direction, respectively. The simulation agrees very well with the calculation, which suggests that the e-e collisions are correctly modeled in the PIC simulation. We can also see from this simulation that it takes more than 50 ps for the plasma to eventually approach the thermal state, which means that for the first

a few ps, the effects of collisions are negligible and the evolution of the anisotropic plasma is dominated by kinetic instabilities. This is also consistent with the result shown in Fig. 5 in the main text. Figure S3B shows the results of a similar simulation where the plasma consists of two group of electrons both with bi-temperature distributions. The densities of the two group of electrons are the same, $n_1 = n_2 = 2.5 \times 10^{18}$ cm$^{-3}$. The temperatures of the electrons in the hot ($\perp$) direction are 214 eV and 60 eV, respectively. The temperature in the orthogonal ($\parallel$) direction is 5 eV. All other parameters are the same as in the previous simulation. The temperatures of each species as functions of time are shown in fig. S3B. Once again, it takes tens of ps for the plasma to thermalize and the effects of collisions in the first few ps are negligible.

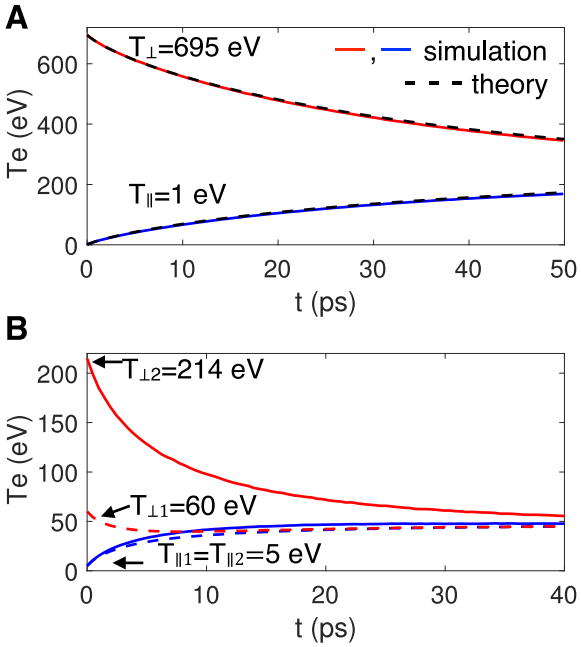


**Fig. S3. Relaxation of nonthermal plasma due to Coulomb collisions.** (**A**) four drifting-Maxwellian beams, (**B**) two bi-temperature beams.

**Recurrence of the streaming mode in the linear polarization case**

An example of the datasets where the streaming mode has a recurrence is shown in fig. S4. Figure S4A shows the raw data of the measured spectra as a function of time. It can be seen that following the first main peak in the blue satellite of the electron feature, there is a second peak at ~3.2 ps. The blue line in fig. S4B shows the measured magnitude of the electron feature (the blue satellite) as a function of time. The red line shows the same simulation result as that in Fig. 6A. Because in this measurement we did not synchronize the pump and probe pulse accurately, there could be a relatively larger uncertainty (comparing to the ~100 fs in Fig. 4) in determining the $t_0$. The measured data is therefore (artificially) shifted by +0.7 ps so that the first peak of the measured data matches that of the simulation. The green line shows the evolution of the magnitude of the measured zero-frequency feature, which shows a similar fixed phase relationship with the electron feature as in Fig. 6.

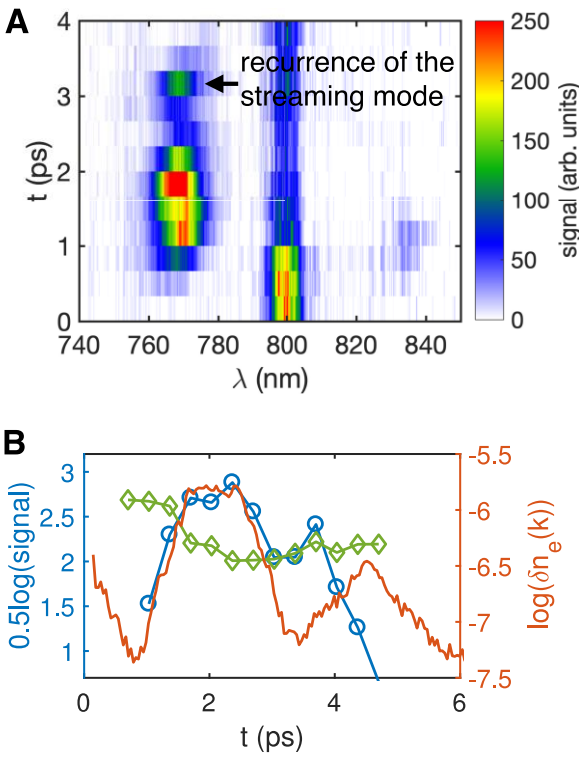


**Fig. S4. Recurrence of the streaming mode and the fixed phase relationship between the streaming and the filamentation modes.** (**A**) Measured spectra at different time delays. (**B**) Comparison between the measured magnitude of the electron feature (blue) as a function of time and the simulation (red). The measured data is artificially shifted by +0.7 ps so that the first peaks of the measured data matches that of the simulation. The green line shows the evolution of the magnitude of the zero-frequency feature, which shows the fixed phase relationship with the electron feature.